

Joint Chance-constrained Game for Coordinating Microgrids in Energy and Reserve Markets: A Bayesian Optimization Approach

Yifu Ding, Benjamin Hobbs

arXiv:2306.12644v1 [math.OC] 22 Jun 2023

Abstract—Microgrids incorporate distributed energy resources (DERs) and flexible loads, which can provide energy and reserve services for the main grid. However, due to uncertain renewable generations such as solar power, microgrids might under-deliver reserve services and breach day-ahead contracts in real-time. If multiple microgrids breach their reserve contracts simultaneously, this could lead to a severe grid contingency. This paper designs a distributionally robust joint chance-constrained (DR-JCC) game-theoretical framework considering uncertain real-time reserve provisions and the value of lost load (VoLL). Leveraging historical error samples, the reserve bidding strategy of each microgrid is formulated into a two-stage Wasserstein-metrics distribution robust optimization (DRO) model. A JCC is employed to regulate the under-delivered reserve capacity of all microgrids in a non-cooperative game. Considering the unknown correlation among players, a novel Bayesian optimization method approximates the optimal individual violation rates of microgrids and market equilibrium. The proposed game framework with the optimal rates is simulated with up to 14 players in a 30-bus network. Case studies are conducted using the California power market data. The proposed Bayesian method can effectively regulate the joint violation rate of the under-delivered reserve and secure the profit of microgrids in the reserve market.

Keyword— Joint chance constraint, Wasserstein-metrics ambiguity set, power market, game theory, Bayesian optimization

I. NOMENCLATURE

A. Set and indices

$t \in \mathcal{T}$	Set, index of time steps
$n \in \mathcal{N}$	Set, index of network buses
$i \in \mathcal{I}$	Set, index of microgrids
$j \in \mathcal{J}$	Set, index of net loads
$k \in \mathcal{K}$	Set, index of thermal generators
$s \in \mathcal{S}$	Set, index of forecast error samples

B. Parameters

N_B	Number of buses
N_S	Number of error samples for constructing ambiguity sets
N_{LN}	Number of lines in the network
N_L	Number of passive loads
N_{MG}	Number of active microgrids

N_{OS}	Number of out-of-sample tests
N_{IT}	Number of iterations in Bayesian optimization
m^g	Fuel cost of thermal generations [\$/ (MWh) ²]
m^s	Battery degradation cost of microgrids [\$/ (MWh) ²]
m^{mgr}	Reserve provision cost of microgrids [\$/MWh]
m^{gr}	Reserve provision cost of thermal generators [\$/MWh]
R^{req}	System reserve requirement [MW]
\overline{P}^g	Power capacity of thermal generators [MW]
P^{nl}	Net loads at buses [MW]
V	VoLL of microgrids [\$/MWh]
\overline{R}^{fup}	Maximum energy capacity of the under-delivered reserve of each microgrid [MWh]
\overline{P}^s	Lower power limit of flexible renewable generations of each microgrid [MW]
\underline{P}^s	Upper power limit of flexible renewable generations of each microgrid [MW]
\overline{L}	Line limit of the transmission network [MW]
ν	Radius of the Wasserstein-metrics ambiguity set
γ	Fraction of flexible generations in microgrids that can be used for reserve provision
ϵ^{jot}	Joint violation rate

C. Variables

π^r	Reserve bidding prices [\$/MWh]
π^e	Energy bidding prices [\$/MWh]
P^g	Power output of thermal generators [MW]
P^s	Power output of flexible generations of microgrids [MW]
P^{inj}	Power injection at each bus [MW]
R^g	Reserve capacity offers of thermal generators [MW]
R^{up}	Reserve capacity offers of microgrids [MW]
P^{ex}	Energy capacity offers of microgrids [MW]
ϵ^{ind}	Individual violation rate
ζ	Uncertain variable for solar forecast errors

II. INTRODUCTION

This paper presents a joint chance-constrained (JCC) game design that facilitates the coordination of renewable microgrids in the bilateral market, ensuring reliable energy and

¹Yifu Ding is with the Massachusetts Institute of Technology Energy Initiative, USA. yifuding@mit.edu

²Benjamin Hobbs is with Whiting School of Engineering, Johns Hopkins University, USA bhobbs@jhu.edu

reserve service provisions. This JCC problem is solved by the Bayesian optimization approach for the first time.

The transition to the net-zero energy system drives the rise of behind-the-meter assets, including solar PV panels, heat pumps, and electric vehicles [1]. However, these assets do not directly receive price signals from the wholesale power or ancillary markets. An organized ancillary services market is normally subject to regulation or bilateral contracts with the system operator, in some cases involving an auction procedure [2]. These distributed energy resources, therefore, could be aggregated as a microgrid to reach the minimum capacity for market participation. Considering these microgrids have no explicit energy and power capacity, they must provide evidence to meet the technical requirements for service provisions and reach an agreement in binding contracts. However, due to weather-dependent renewable generations and stochastic demands, under-delivered services and contract breaches might occur, which undermines system reliability in responses to grid contingencies.

To coordinate their energy service provisions, different market designs have been proposed, including distribution locational marginal prices (DLMPs) [3], [4], bilateral matching [5], and game-theoretical framework [6], [7]. The LMP and bilateral matching frameworks consider microgrids as price-takers, meaning they do not influence the market, such as other participants' strategies. Game-theoretical frameworks are usually employed to simulate a competitive procedure such as auctions, where market participants have their own objectives, and their biddings change depending on risk appetites and the market environment until an equilibrium is reached. This market dynamics can be modeled mainly by either of two methods. They are the iterative or heuristic algorithm to search for the equilibrium, such as the best response algorithm, and mathematical programming with equilibrium constraints (MPEC) [8].

The first method simulates each player's strategy iteratively and searches a market equilibrium until all players' solutions converge to a global optimum [9], [10]. However, this approach only guarantees convergence to an efficient equilibrium for certain types of utility functions, and it is sensitive to the starting point [11]. MPEC method based on Karush-Kuhn-Tucker (KKT) rule secures the equilibrium when at least a feasible solution exists, but it results in the non-convex optimization problem requiring additional mathematical reformulations [12].

In a competitive framework like auctions, the interactions between ISO and microgrids (or distribution system operators (DSOs)) are often simulated by two types of games, the Stackelberg and Nash bargaining games. The Stackelberg game models the relatively small and passive consumers w.r.t. the market, assuming they cannot affect the price [13], [7]. In contrast, the Nash bargaining game could model the large consumers who can negotiate prices and impact the market [14], [15]—for example, ref. [15] models the interactions of aggregators and demand response providers. This work shows that the existing outcome of a Stackelberg Game between the aggregator and consumers is a subset of the set of possible outcomes of a Nash Bargaining Game, where the consumer

has the bargaining power.

When engaging in the market game, it is essential to consider uncertainty from both the generation and demand sides, alongside the risk tolerance of participants. The scenario-based approach is a straightforward way to model uncertainty. Uncertain scenarios can be generated for stochastic renewable generations [13], [10], and imperfect reserve provisions for service calls [7]. However, the computation cost of the scenario-based approach increases with the number of scenarios. This becomes a significant bottleneck if the model tries to model the individual characteristics of a great number of game players.

An alternative method is introducing the analytical approach, such as the chance-constrained (CC) [15], conditional value-at-risk (CVaR) [16], and distributionally robust formulations [17]. These formulations assume an underlying distribution or a family of distributions for uncertain variables and model the expected market outcomes at a certain chance. This allows the introduction of risk-aware metrics such as the confidence level of power generation and energy service provision failure rates [18], [19]. The players' strategies are interlinked in a game, and the market equilibrium is considered the joint solution of all players. Therefore, to model the simultaneous occurrence of multiple players' strategies considering uncertainty in a game, a JCC formulation is required.

The JCC problem generally cannot be solved directly. However, their solutions can be approximated by decomposing the JCC into tractable single CCs and enforcing *Boole's inequality*, meaning that the chance that at least one of the events happens is no greater than the sum of the possibilities of all individual events. A particular case is the *Bonferroni approximation*, which assumes that these CCs are entirely independent and the sum of individual violation rates is equal to the joint violation rate [17], [20]. However, CCs with the same uncertainty source (e.g., renewable power sources within an area) are usually positively correlated. This assumption neglects their correlation and increases solution conservativeness. Ref. [20] proves the solution conservativeness of the JCC problem will increase with the number of decomposed CCs if their violation rates are obtained using the *Bonferroni approximation*. Furthermore, ref. [21] proves that if these constraints tend to be completely correlated, the efficacy of the *Bonferroni approximation* will diminish.

Although the correlation of decomposed CCs is impactful in a JCC problem, this topic has received very limited discussions in the existing game designs. Ref. [18] first used the JCC formulation in a Nash-Cournot game to simulate the impact of uncertain wind power outputs in the electricity market considering the congestion arbitrage. This work found that the profits of wind farms largely depend on the confidence level of wind power generation predictions. However, it simply assumes all the wind farms are independent and have the same confidence levels in predictions. Recent work [10] uses a DRJCC formulation to model the generalized Nash equilibrium problem for coordinating the renewable energy aggregators in the local electricity market. The work considers the maximum power outputs of aggregators as an uncertain distribution. Then the model solves their bidding strategies

and market equilibrium using the best response algorithm. Nevertheless, all renewable energy aggregators are assumed to have the same risk attitudes, and the correlation between players' decisions is not discussed in the paper, even though the game is simulated with varying numbers of players.

To identify the correlation between CCs and reduce solution conservativeness, a common method is pre-solving the problem with a conservative guess, then progressively tightening the worst-case bounds. For example, ref. [21] proposed a tractable CVaR formulation to model the worst-case bound of the JCC problem. An auxiliary variable is introduced to tighten the bound and solved iteratively with decision variables. This optimized CVaR method has been applied in the energy and reserve joint dispatch problem [16]. Refs. [22] and [23] solve the JCC optimal power flow (OPF) problem. To obtain a low-conservative solution, they estimate analytically and eliminate the overlapped violation events due to the correlated CCs in an iterative framework. Both effectively reduce solution conservativeness but require a comprehensive analysis of violation events in the network. Recent work [24] incorporates the correlation in power generations of wind farms in the ambiguity set as a constraint in the DRO formulation. However, this requires the specified correlation that is hard to obtain in a changing power market environment.

This paper designs a DRJCC game framework to coordinate solar-powered microgrids in the energy and reserve markets and proposes a novel Bayesian approach to approximate the optimal solution. Compared with stochastic game designs in the existing literature, our contributions are two-fold,

(i) From the perspective of the market design, a two-stage DRO formulation is employed to model the risk-aware bidding of microgrids, considering the worst-case reserve provision performance. In accordance with the existing market design in the U.S., the penalty due to the under-delivered reserve is modeled on the microgrids' side, and a system regulation to manage the day-ahead reserve contract breach is imposed by the system operator. The interactions of the system operator and multiple microgrids in the power markets are simulated in a Stackelberg leader-follower game.

(ii) From the perspective of the algorithm design, a JCC regulates the under-delivered reserve of all microgrids jointly, while the correlation among players is unknown in a changing market game. To avoid an over-conservative reserve regulation, a novel Bayesian optimization method is proposed and applied to approximate individual contract violation rates of decomposed DRCCs. Compared with the latest work [25], it is the first attempt to use Bayesian optimization to solve the DRJCC problem.

III. DRJCC MARKET GAME CONSIDERING UNCERTAIN RESERVE PROVISION

This market game is simulated in the two-settlement electricity market, which consists of a day-ahead market and a real-time market. We use a bilevel optimization framework to model the interactions of the independent system operator (ISO) and contracted microgrids in the market pool.

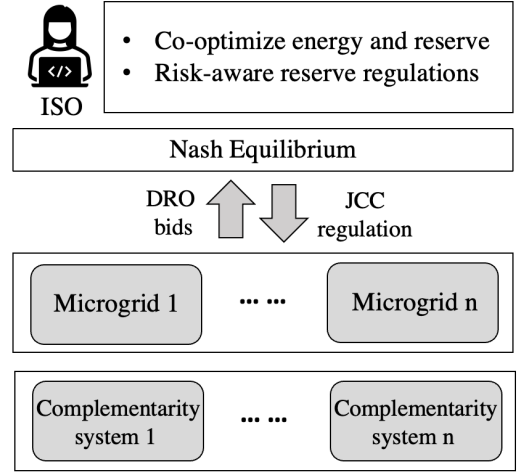


Fig. 1: Bilevel game framework for ISO and contracted microgrids

A. Players

This game includes two types of players, ISO as a leader and contracted microgrids as followers. As shown in Fig.1, ISO manages the transmission network and market pool. In the day-ahead market, ISO sets energy and reserve requirements using probabilistic net load forecasts (i.e., power demands subtracting solar power generations) at network nodes. ISO receives reserve offers from thermal generators and microgrids and signs day-ahead contracts.

However, due to renewable generation uncertainty, reserve services from renewable microgrids might under-deliver in real time. To guarantee system reliability, ISO needs to analyze the reserve provision performance, regulate contract violations in the market pool, and broadcast the individual violation allowance to microgrids. Meanwhile, to avoid penalty and payment reduction, each microgrid can leverage the historical forecast data and adjusts its risk appetite in bidding.

B. Game type

This game is a one-leader-multiple-follower Stackelberg game. In this type of game, the leader anticipates followers' actions and moves first, while followers take actions afterward only based on the leader's move. In our work, ISO knows all the bids from microgrids (e.g., capacity, penalty, and risk appetite) and conducts the market clearing. Each microgrid bids only based on the market clearing result without knowing other players' bidding strategies. Microgrids are assumed to be small-scale consumers who do not affect prices.

IV. MODEL FORMULATION

We first formulate the optimization for ISO and microgrids. To model their interactions, we integrate these optimization models into a complementarity model that can represent the simultaneous optimization problems of one, or several decision-makers [26]. Leveraging the DRJCC formulation, we model uncertain reserve provisions performance of microgrids and the reserve regulation by ISO.

A. Wasserstein-metric ambiguity set to model the worst-case reserve performance

Assuming that microgrids are mainly supplied by renewable power sources such as solar panels or wind farms, their real-time reserve provision performances are modeled based on historical renewable forecast error samples. We use historical error samples to construct a Wasserstein-metric ambiguity set and model the worst-case reserve performance. The Wasserstein-metric ambiguity set is a moment-free method without any underlying distribution assumptions, which could leverage the empirical data effectively. It constructs a ball-shape set space which allows adjusting conservativeness by a radius. We chose the Wasserstein distance due to its advantages, including symmetry and the ability to capture the worst-case distribution [27].¹

Let the error sample vector $\mathbf{s} := \{s_1, s_2, \dots, s_n\}$ be a vector including n random samples of the uncertain variable ζ at time interval t . If $s_1 \sim \mathbb{P}_1$ and $s_2 \sim \mathbb{P}_2$, the Wasserstein metric $W(\mathbb{P}_1, \mathbb{P}_2)$ between two distributions \mathbb{P}_1 and \mathbb{P}_2 is given by [29],

$$W(\mathbb{P}_1, \mathbb{P}_2) = \inf_{\mathcal{Q} \in \mathcal{R}(\Xi)} \left\{ \int \|s_1 - s_2\| \mathcal{Q}(ds_1, ds_2) \right\} \quad (1)$$

The term $\|s_1 - s_2\|$ is the distance between two samples, and $\mathcal{Q}(ds_1, ds_2)$ is the joint distribution with marginal distributions \mathbb{P}_1 and \mathbb{P}_2 on the support $\mathcal{R}(\Xi)$. The Wasserstein-metric ambiguity set \mathcal{P} is a ball space of radius $\nu \geq 0$ concerning Wasserstein distance, centered at a prescribed reference distribution \mathbb{P}_ζ based on samples \mathbf{s} .

$$\mathcal{P} := \{\mathbb{P} : \mathbb{P} \in \mathcal{R}(\Xi), W(\mathbb{P}, \mathbb{P}_\zeta) \leq \nu\} \quad (2)$$

This work uses historical error samples of solar power forecasts from California independent system operator (CAISO) during 2021 and 2022 [30].

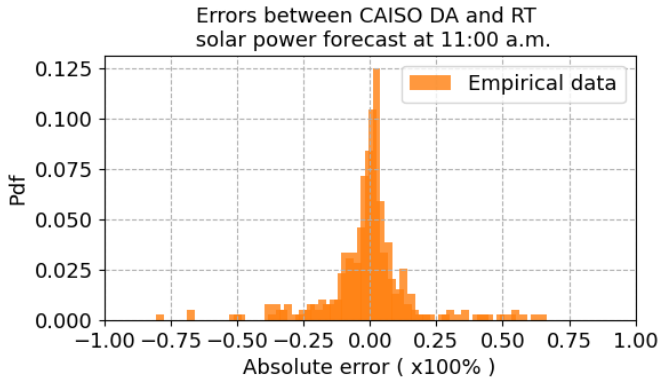


Fig. 2: The solar power forecast error distribution between DAM and RTM at 11:00 a.m.[30]

We choose two real-time market intervals at 15 and 45 mins in each hour to calculate these errors between DAM and RTM.

¹Other moment-free distances, such as KL-divergence, can also be employed theoretically. However, it is an asymmetric metric, meaning that the divergence from the distribution \mathbb{P} to \mathbb{Q} is not equal to the divergence from the distribution \mathbb{P} to \mathbb{Q} [28]. This will bring more complexity in defining conservativeness.

Fig. 2 shows the calculated error distribution at 11:00. For each time interval, we choose $N_S = 200$ to construct the ambiguity set. These error samples are integrated into the model as a matrix $\mathbf{s} \in \mathbb{R}^{N_S \times N_T}$.

B. ISO's optimization problem for the energy and reserve joint dispatch

This work considers a power network with N_B buses and N_{LN} lines. Its bus susceptance matrix denotes as $\mathbf{B}_{bus} \in \mathbb{R}^{N_B \times N_B}$. Flow susceptance matrix denotes as $\mathbf{B}_{line} \in \mathbb{R}^{N_{LN} \times N_B}$ to calculate the difference in voltage angle across each line. Thermal generations, loads, and microgrids are located on different buses. Their positions in the network are mapped by sparse matrices $\mathbf{C}^g \in \mathbb{R}^{N_B \times N_G}$, $\mathbf{C}^l \in \mathbb{R}^{N_B \times N_L}$ and $\mathbf{C}^{mg} \in \mathbb{R}^{N_B \times N_{MG}}$. All the vectors in **bold** without specification represent the vector of a variable or a parameter across the network over the optimization horizon (e.g., \mathbf{P}^{nl} is all the net loads over the period \mathcal{T}). Given a real-time market clearing interval $\Delta t \in \mathcal{T}$, the multi-period power dispatch considering the network is formulated as follows.

1) *The objective function*: The cost function consists of two parts: the first part is the cost of energy and reserve provision from thermal power plants, and the second part is the profit from the energy and reserve market, which is the product of bidding price and quantity.

$$(M1) \min \mathcal{J}^H = \min \left\{ \sum_{t \in \mathcal{T}} \sum_{k \in \mathcal{K}} (m_k^g (\Delta t P_{t,k}^g)^2 + \Delta t m_k^{gr} R_{t,k}^g) + \sum_{t \in \mathcal{T}} \sum_{i \in \mathcal{I}} \Delta t (\pi_i^r R_{t,i}^{up} - \pi_i^e P_{t,i}^{ex}) \right\} \quad (3)$$

2) *Power and reserve balances*: Power balance is required, and the total reserve capacity offer must be greater than the reserve requirement.

$$\sum_{k \in \mathcal{K}} P_{t,k}^g + \sum_{i \in \mathcal{I}} P_{t,i}^{ex} = \sum_{j \in \mathcal{J}} P_{t,j}^{nl} \quad t \in \mathcal{T} \quad (4)$$

$$\sum_{i \in \mathcal{K}} R_{t,k}^g + \sum_{i \in \mathcal{I}} R_{t,i}^{up} \geq R_t^{req} \quad t \in \mathcal{T} \quad (5)$$

Energy and reserve provisions are non-negative, and the sum should be less than the power capacity.

$$\mathbf{P}^g + \mathbf{R}^g \leq \overline{\mathbf{P}}^g \quad (6)$$

$$\mathbf{P}^g \geq 0, \mathbf{R}^g \geq 0 \quad (7)$$

3) *Power injections and line limits*: The net power injection is the sum of thermal power generations, reserve provisions, load consumptions, or power exchanged with microgrids at each node.

$$\mathbf{P}^{inj} = \mathbf{C}^g (\mathbf{P}^g + \mathbf{R}^g) - \mathbf{C}^{mg} (\mathbf{P}^{ex} - \mathbf{R}^{up}) - \mathbf{C}^l \mathbf{P}^{nl} \quad (8)$$

Power flow is regulated within the thermal power capacity of each line.

$$\mathbf{B}_{line} \mathbf{B}_{bus}^{-1} \mathbf{P}^{inj} \leq \overline{\mathbf{L}} \quad (9)$$

$$\mathbf{B}_{line} \mathbf{B}_{bus}^{-1} \mathbf{P}^{inj} \geq -\overline{\mathbf{L}} \quad (10)$$

4) *Reserve performance regulations based on day-ahead contracts*: ISO regulates the reserve performance based on their day-ahead contracts. If multiple microgrids fail to deliver reserve service simultaneously, it might lead to a severe grid contingency. ISO regulates the occurrence of these violation events. We formulate this as a JCC considering the Wasserstein-metric ambiguity set \mathcal{P} . If the maximum under-reserved capacity $\overline{R^{fup}}$ is agreed in each day-ahead contract, the JCC is given by,

$$\inf_{\mathbb{P} \in \mathcal{P}} \mathbb{P}\left(\bigcap_{i \in \mathcal{I}} \left\{ \sum_{t \in \mathcal{T}} \Delta t \zeta R_{i,t}^{up} \leq \overline{R^{fup}} \right\}\right) \geq 1 - \epsilon^{jot} \quad (11)$$

ϵ^{jot} represents the occurrence of joint contract violation. This is a predetermined parameter and depends on grid conditions. To assess the performance of each microgrid, the JCC (11) is decomposed into single CCs for individual contracts considering unspecified correlation.

$$\inf_{\mathbb{P} \in \mathcal{P}} \mathbb{P}\left(\sum_{t \in \mathcal{T}} \Delta t \zeta R_{i,t}^{up} \leq \overline{R^{fup}}\right) \geq 1 - \epsilon_i^{ind} \quad i \in \mathcal{I} \quad (12)$$

ϵ_i^{ind} represents the maximum chance of breaching individual contracts. This will be optimized and broadcast to each microgrid as regulations, depending on the total contracts in the market pool.

$$\epsilon_i^{ind} \in \left[\frac{\epsilon^{jot}}{N_{MG}}, \epsilon^{jot} \right] \quad (13)$$

Since the correlation among players are unknown, ϵ_i^{ind} could not be solved directly. Instead, we could estimate its value within a range. We consider two extreme scenarios as the range (13). The lower bound (i.e., $\frac{\epsilon^{jot}}{N_{MG}}$) is based on the *Bonferroni approximation*. In this case, assuming no correlation among microgrids, decomposed CCs have the same violation rate divided equally from the joint violation rate. The upper bound (i.e., ϵ^{jot}), on the contrary, assumes all microgrids are completely correlated and have the same reserve provision performance.

5) *CVaR approximation and reformulation*: As the proof (Theorem 2.2) in ref. [31], each DRCC (12) can be approximated as a CVaR constraint and then reformulated into the following convex constraints based on refs. [32], [33].

$$-\eta_i^u - \frac{1}{\epsilon_i^{ind}} \left(\nu l_i^u + \frac{\mathbf{1}^\top \mathbf{W}_i^u}{N_S} \right) \geq 0 \quad (14)$$

$$\mathbf{W}_i^u - \Delta t \mathbf{s} (\mathbf{R}_i^{up})^\top + \overline{R^{fup}} + \eta_i^u \geq 0 \quad (15)$$

$$\mathbf{W}_i^u \geq 0 \quad (16)$$

$$\|\Delta t \mathbf{s} (\mathbf{R}_i^{up})^\top\| \leq l_i^u \quad (17)$$

The matrices $\mathbf{R}_i^{up} \in \mathbb{R}^{1 \times N_T}$ and $\mathbf{s} \in \mathbb{R}^{N_S \times N_T}$ denote the reserve vector of microgrid i and the empirical reserve forecast error matrix. The variables η^u , l^u , $\mathbf{W}^u \in \mathbb{R}^{N_S \times 1}$ are auxiliary variables.

C. *Data-driven bidding strategy considering the worst-case reserve performance*

Microgrids schedule their energy and reserve bids in a risk-aware manner leveraging historical forecast error data. A two-stage DRO model is used for data-driven bidding. The first stage models the energy and reserve schedule in the day-ahead market, and the second stage models the expected penalty of under-delivered reserve considering the worst-case error distributions. The penalty depends on the empirical error samples and day-ahead reserve bids at the first stage. The following subsections present the optimization model for each microgrid $i \in \mathcal{I}$.

1) *The objective function*: The cost of each microgrid includes three parts. The first part is the cost of energy and reserve provisions, and the second is the revenue from energy and reserve service trading. The final part models the economic penalty due to the unavailable reserve service. Here we assume the penalty as the expected load-shedding loss in the worst case, using the DRO formulation based on the Wasserstein-metric ambiguity set \mathcal{P} .

$$(M2) \min \mathcal{J}^L = \min \left\{ \sum_{t \in \mathcal{T}} (m_i^s (\Delta t P_{i,t}^s)^2 + \Delta t m_i^{mgr} R_{i,t}^{up} + \Delta t \pi_i^e P_{i,t}^{ex} - \Delta t \pi_i^r R_{i,t}^{up}) \right\} + \sup_{\mathbb{P} \in \mathcal{P}} [\Delta t \zeta R_{i,t}^{up} V_i] \quad (18)$$

The load-shedding loss due to the under-delivered reserve is calculated by multiplying the under-delivered reserve capacity and the per-unit VoLL (i.e., V_i) of each microgrid.

2) *Convex reformulation of DRO*: The DRO term in the objective function can be reformulated, as Corollary 5.4 in ref. [32].

$$\sup_{\mathbb{P} \in \mathcal{P}} \mathbb{E} \left[\sum_{t \in \mathcal{T}} \Delta t \zeta R_{i,t}^{up} V_i \right] = \nu l_i^l + \frac{\mathbf{1}^\top \mathbf{W}_i^l}{N_S} \quad (19)$$

$$(\boldsymbol{\mu}^{dro1}) \quad \mathbf{W}_i^l - \Delta t \mathbf{s} (\mathbf{R}_i^{up})^\top V_i + \eta_i^l \geq 0 \quad (20)$$

$$(\boldsymbol{\mu}^{dro2}) \quad \mathbf{W}_i^l \geq 0 \quad (21)$$

$$(\boldsymbol{\mu}^{dro3}) \quad \Delta t \mathbf{s} (\mathbf{R}_i^{up})^\top V_i + l_i^l \geq 0 \quad (22)$$

$$(\boldsymbol{\mu}^{dro4}) \quad \Delta t \mathbf{s} (\mathbf{R}_i^{up})^\top V_i - l_i^l \leq 0 \quad (23)$$

where l^l , η^l and $\mathbf{W}^l \in \mathbb{R}^{N_S \times 1}$ are auxiliary variables in the reformulation. The dual variables in the bracket, $\boldsymbol{\mu}^{dro1}$, $\boldsymbol{\mu}^{dro2}$, $\boldsymbol{\mu}^{dro3}$ and $\boldsymbol{\mu}^{dro4}$ all have the same dimension $\mathbb{R}^{N_S \times 1}$.

3) *Power balance and provision*: Each microgrid requires power balance. Power sources in microgrids are considered flexible power generations, which consist of renewable power sources and energy storage (ES). Microgrids can thus import and export power. In the power markets, ISO can only know energy and reserve offers from microgrids instead of their dispatch. Therefore, this model does not include the energy constraints of ES and the power flow for each microgrid.

$$(\boldsymbol{\mu}^{pb}) \quad P_{i,t}^{ex} + P_{i,t}^s = P_{i,t}^{nl} \quad t \in \mathcal{T} \quad (24)$$

$$(\boldsymbol{\mu}^{dnpl}, \boldsymbol{\mu}^{uppl}) \quad -\underline{P}^s \leq P_{i,t}^s \leq \overline{P}^s \quad t \in \mathcal{T} \quad (25)$$

4) *Reserve provision*: The upper limit of reserve provision is set as a fraction of the flexible power generation level.

$$(\boldsymbol{\mu}^{dnrl}, \boldsymbol{\mu}^{uprl}) \quad 0 \leq R_{i,t}^{up} \leq \gamma P_{i,t}^s \quad t \in \mathcal{T} \quad (26)$$

D. Complementarity model for market equilibrium

ISO and microgrids' optimization are interlinked in the quantity of energy and reserve capacity offers (i.e., $\pi^r R^{up} - \pi^e P^{ex}$). To form a one-leader-multiple-follower problem, the MPEC technique is employed to solve two types of optimizations simultaneously and obtain market equilibrium. Based on the strong duality and KKT rule, the dual problem of model M2 is formulated and integrated into the upper-level model, model M1. We have N_{MG} of microgrids in the game over the period \mathcal{T} . We omit the indexes i, t for conciseness. $\mathbf{1}^s$ represents a unit vector with the same dimension as the error sample vector \mathbf{s} .

First, stationary constraints are formulated for six decision variables $P^s, P^{ex}, R^{up}, l^l, W^l$ and η^l in model M2.

$$2\Delta t m^s P^s + \mu^{pb} - \mu^{dnpl} + \mu^{uppl} - \gamma \mu^{uprl} = 0 \quad (27)$$

$$\pi^e + \mu^{pb} = 0 \quad (28)$$

$$\Delta t (m^{mgr} - \pi^r) + \Delta t \mathbf{s}^\top (\boldsymbol{\mu}^{dro1} - \boldsymbol{\mu}^{dro3} + \boldsymbol{\mu}^{dro4}) V - \mu^{dnrl} + \mu^{uprl} = 0 \quad (29)$$

$$\nu - (\mathbf{1}^s)^\top \boldsymbol{\mu}^{dro3} - (\mathbf{1}^s)^\top \boldsymbol{\mu}^{dro4} = 0 \quad (30)$$

$$\frac{1}{N_S} - \boldsymbol{\mu}^{dro1} - \boldsymbol{\mu}^{dro2} = 0 \quad (31)$$

$$(\mathbf{1}^s)^\top \boldsymbol{\mu}^{dro1} = 0 \quad (32)$$

Complementary slackness constraints are,

$$0 \leq (\mathbf{W}^l - \Delta t \mathbf{s} (\mathbf{R}^{up})^\top V + \eta^l) \perp \boldsymbol{\mu}^{dro1} \geq 0 \quad (33)$$

$$0 \leq \mathbf{W}^l \perp \boldsymbol{\mu}^{dro2} \geq 0 \quad (34)$$

$$0 \leq (\Delta t \mathbf{s} (\mathbf{R}^{up})^\top V + l^l) \perp \boldsymbol{\mu}^{dro3} \geq 0 \quad (35)$$

$$0 \leq (l^l - \Delta t \mathbf{s} (\mathbf{R}^{up})^\top V) \perp \boldsymbol{\mu}^{dro4} \geq 0 \quad (36)$$

$$0 \leq (\overline{P^s} - P^s) \perp \mu^{uppl} \geq 0 \quad (37)$$

$$0 \leq (\underline{P^s} + P^s) \perp \mu^{dnpl} \geq 0 \quad (38)$$

$$0 \leq R^{up} \perp \mu^{dnpl} \geq 0 \quad (39)$$

$$0 \leq (\gamma P^s - R^{up}) \perp \mu^{uppl} \geq 0 \quad (40)$$

Constraints (33) - (40) are non-linear. We thus use the big-M technique. Assuming a and b are variables, the non-linear constraint on the left-hand side can be transformed into the four convex constraints on the right-hand side.

$$0 \leq a \perp b \geq 0 \Rightarrow a \geq 0, b \geq 0, a \leq MU, b \leq M(1-U) \quad (41)$$

where M is a number far larger than a and b , and U has the same dimension as a and b .

The objective function of ISO's optimization problem is nonlinear after reformulation, as it has a multiplication of price and capacity variables. We linearize it based on the strong duality theory. The reformulated model for solving the market equilibrium of ISO and N_{MG} of microgrids is as follows.

$$(M3) \quad \min_{\Xi_{bi}} \mathcal{J} = \min \left\{ \sum_{t \in \mathcal{T}} \sum_{k \in \mathcal{K}} (m_k^g (\Delta t P_{t,k}^g)^2 + \Delta t m_{t,k}^{gr} R_{t,k}^g) \right. \\ \left. + \sum_{t \in \mathcal{T}} \sum_{i \in \mathcal{I}} [m_i^s (\Delta t P_{t,i}^s)^2 + \Delta t m_i^{mgr} R_{t,i}^{up} + (\nu l_i^l + \frac{\mathbf{1}^\top \mathbf{W}_i^l}{N_S} \right. \\ \left. - \Delta t \mu_{t,i}^{pb} P_{t,i}^l + \Delta t \mu_{t,i}^{uppl} \overline{P^s} + \Delta t \mu_{t,i}^{dnpl} \underline{P^s})] \right\} \\ \text{s.t. equations (4) - (17) and (27) - (40)} \quad (42)$$

where the variable set Ξ_{bi} includes $P^g, R^g, P^s, R^{up}, R^{ex}, \pi^r, \pi^e, l^l, \eta^l, \mathbf{W}^l, \eta^u, l^u, \mathbf{W}^u, \epsilon^{ind}, \mu^{dro1}, \mu^{dro2}, \mu^{dro3}, \mu^{dro4}, \mu^{pb}, \mu^{dnpl}, \mu^{uppl}, \mu^{dnrl}, \mu^{uprl}$.

V. APPROXIMATING THE OPTIMAL SOLUTIONS USING BAYESIAN OPTIMIZATION

The reformulated model M3 is intractable with unknown optimal individual violation rates ϵ^{ind} . We introduce Bayesian optimization to approximate the optimal solution iteratively. The target black-box function is thus the unspecified relationship between ϵ^{ind} and ϵ^e , $\epsilon^e = \mathcal{F}(\epsilon^{ind})$. Bayesian optimization is a global approximation approach to optimize the black-box function. Its applications include hyper-parameter tuning for deep learning models [34] and solving difficult combinatorial optimizations [35]. Bayesian optimization best suits the expensive-to-evaluate functions and tolerates the stochastic noise in function evaluations [35].

Bayesian optimization is thus introduced to solve the black-box function, given the following two reasons: First, the black-box function cannot be explicitly computed. Its evaluation process requires out-of-sample tests, which are considered to have noisy observations. Second, during the optimization process, we do not consider data transfer costs, which can be substantial if the power network scales up. Bayesian optimization can guarantee performance within a limited number of iterations and reduce evaluation costs. The following subsections summarize its algorithm, the design of the evaluation, and acquisition functions in the process.

A. Summary of the algorithm

Algorithm 1: Solving M3 using Bayesian optimization

```

Initialize model M3 and define the exploration space;
Evaluate the initial samples  $\epsilon_o$ ;
for  $m = 1, \dots, N_{IT}$  do
    Update the surrogate model with observations  $\mathbf{O}_m$ ;
    Identify new samples  $\epsilon_{m+1} = \text{argmax} \mathcal{G}(\epsilon_m; \mathbf{O}_m)$ ;
    Query the evaluation function  $\mathcal{H}(\epsilon_{m+1})$ ;
    Augment observations
     $\mathbf{O}_{m+1} := \{\mathbf{O}_m; (\epsilon_{m+1}, \mathcal{H}(\epsilon_{m+1}))\}$ ;
end

```

As in Algorithm 1, we first initialize the problem to solve, model M3, and define the exploration space of the individual violation rates $\epsilon_m \in [\frac{\epsilon^{jot}}{N_{MG}}, \epsilon^{jot}]$. The dimension of the sample vector is N_{MG} , and the bounds ensure that the black-box function is feasible and continuous over the space. Then, a Gaussian process regressor (GPR) is used as the

surrogate model for fitting the unknown block-box function \mathcal{F} within N_{IT} iterations. GPR assumes a prior distribution for the approximated value $\mathbb{P}(\epsilon_m)$. Given the distributions of observations $\mathbb{P}(\mathbf{O}_m)$ and the likelihood $\mathbb{P}(\mathbf{O}_m|\epsilon_m)$ (i.e., the maximum difference between the estimation and the ground truth), the posterior of GPR (i.e., the probability distribution of the approximated value) is defined as,

$$\mathbb{P}(\epsilon_m|\mathbf{O}_m) = \frac{\mathbb{P}(\mathbf{O}_m|\epsilon_m)\mathbb{P}(\epsilon_m)}{\mathbb{P}(\mathbf{O}_m)} \quad (43)$$

In each iteration m , the posterior is updated using all observations \mathbf{O}_m . After that, new samples are proposed for the next iteration using the acquisition function $\mathcal{G}(\epsilon_m; \mathbf{O}_m)$. These samples are evaluated in the function $\mathcal{H}(\epsilon_{m+1})$ and added to the observation \mathbf{O}_{m+1} . This procedure is executed for N_{IT} iterations.

B. Evaluation of the black-box function

We aim to find the optimal individual violation rates ϵ_m^{ind} so that the empirical outcome ϵ_m^e is as close as to the predefined requirement ϵ^{jot} . As the black box function \mathcal{F} cannot be explicitly computed, an evaluation function $\mathcal{H}(\epsilon_m)$ is proposed to assess results in each iteration and defined as the absolute difference between the empirical and predefined joint violation rates.

$$\mathcal{H}(\epsilon_m) = |\epsilon_m^e - \epsilon^{jot}| \quad (44)$$

Where the empirical joint violation rate ϵ_m^e is obtained from $N_{OS} = 150$ independent out-of-sample tests. In each test, we use an error sample s different from those in the ambiguity set and calculate the under-delivered reserve $R_s^{under} := \Delta t s (\mathbf{R}^{up})^\top$ for each microgrid. A violation event is when any microgrid violates the reserve regulation (i.e., constraint (12)). The empirical joint violation rate is calculated as the ratio of violation events to the total number of tests.

$$\epsilon_m^e := \frac{\sum_{s=0}^{N_{OS}} \mathbb{1}_{(R_s^{under} > \overline{R^{up}})}}{N_{OS}} \quad (45)$$

C. Sample selection using the acquisition function

The acquisition function decides the new sample in the iteration m . Different acquisition functions include the lower confidence bound, the probability of improvement, and the expected improvement [36]. We choose the expected improvement after experiments considering the explore-exploit tradeoff. The function is the maximum expected improvement at the sample ϵ_m estimated from all out-of-sample tests.

$$\mathcal{G}(\epsilon_m; \mathbf{O}_m) = \mathbb{E}[\mathcal{H}' - \mathcal{H}(\epsilon_m)]^+ \quad (46)$$

Where $[\cdot]^+ = \max\{\cdot, 0\}$, and \mathcal{H}' denotes the minimum value obtained in the evaluation function. (46) defines the maximum expected improvement based on the posterior distribution in each iteration, which is greater than 0. Then, a new sample in the next iteration is selected, which gives the maximum value of (46).

$$\epsilon_{m+1} = \underset{\epsilon}{\operatorname{argmax}} \mathcal{G}(\epsilon_m; \mathbf{O}_m) \quad (47)$$

VI. CASE STUDIES

Two case studies are developed using IEEE 30-bus network [37]. As shown in Fig. 3, the power network consists of passive loads and proactive microgrids, marked in black arrows and orange stars, respectively. Each microgrid has a 2MW load on average, a 2MW solar PV generation, and 3MW/6MWh ES system. The parameters of the game framework and Bayesian optimization are presented in Table I.

TABLE I: The parameters of the game framework and Bayesian optimization

		$\overline{R^{up}}$	1.5 MWh	Δt	0.5 hour
m_s	\$1/(MWh) ²	$\overline{P^s}$	3 MW	N_{OS}	150
m_g	\$1/(MWh) ²	γ	0.5	N_{IT}	20
m_{gr}	\$15/MWh	ϵ^{jot}	0.2	N_S	200
$m_{m,gr}$	\$5/MWh				

Net-load profiles are taken from the UK power networks trial [38] and the deep learning model in ref. [39] generates their probabilistic forecasting profiles for reserve requirements. Fig. 4 shows the net load forecast and system reserve requirements. Due to solar power and peak loads, reserve requirements are higher from 6 a.m. to 6 p.m. We choose the reserve requirement R^{req} at the reliability level of 90%.

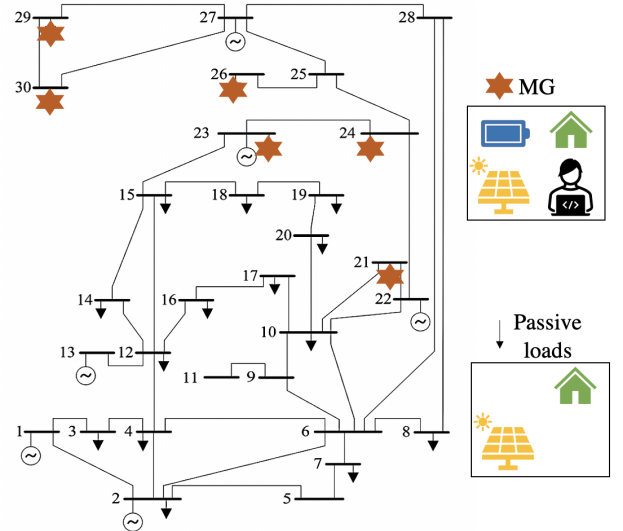


Fig. 3: The 30-bus power network with microgrids

The first case study simulates the game framework with a fixed number of six microgrids. As shown in Fig. 3, microgrids 1-6 are located at buses 21, 23, 24, 26, 29, and 30, respectively. Microgrids 1 and 2 at buses 21 and 23 have a higher VoLL of \$20/MWh, and the rest of the four microgrids have a VoLL of \$1/MWh. We conduct the simulations with different radii of the Wasserstein-metrics ambiguity set \mathcal{P} and aim to find the optimal radius given the predefined requirement ϵ^{jot} . Based on the optimal radius, the second case study simulates the game framework under the varying number of microgrids, ranging from 2 to 14. The correlation of these microgrids changes as the number of players changes. All the microgrids have the same VoLL of \$1/MWh.

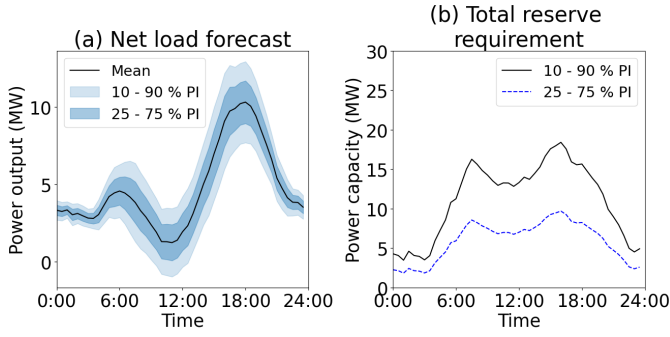


Fig. 4: (a) An example of probabilistic net load forecast at one bus and (b) total reserve procurement requirements at the reliability levels of 75% and 90%

VII. NUMERICAL RESULTS

The proposed DRJCC game framework is simulated for six hours from 6:00 a.m. to 12:00 a.m. This game framework is built using CVXPY package [40] in Python, and the Bayesian optimization is implemented using the scikit-optimize package [41]. The following subsections present results and analysis of two case studies.

A. The optimal radius of Wasserstein-metrics ambiguity sets

The radii of the Wasserstein-metrics ambiguity determines solution conservativeness. The radii of ambiguity set are the choice of ISO and microgrids, which decides the conservativeness of the system reserve regulation. It can be chosen based on grid conditions and system security requirements. In the first case study, we conduct simulations with an increasing radius ranging from 10^{-5} to 10^{-1} to find the optimal radius at the given joint violation rate. For comparison, we simulate the benchmark case where there is no system-wise reserve regulation for all contracts, in other words, disabling constraints (11) - (17).

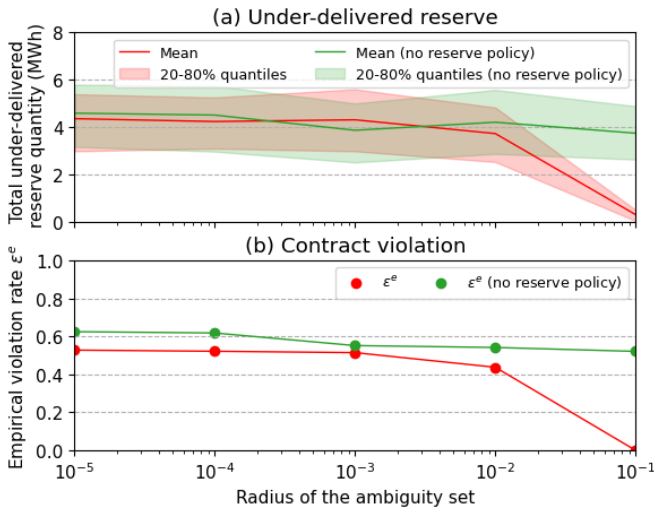


Fig. 5: (a) The total amount of under-delivered reserve and (b) the empirical contract violation rates with an increasing radius of the ambiguity set

Fig. 5 shows the under-delivered reserve and joint violation rates from $N_{OS} = 150$ out-of-sample tests. The red line is the mean value of the under-delivered reserve from all tests, and the red shade shows the 20-80% quantile. The proposed game framework is effective when the radius is between 10^{-2} and 10^{-1} , where the game results differ from the benchmark case (i.e., no reserve policy) significantly. We choose an optimal radius of $\nu = 0.035$ for a joint contract violation rate of 0.2.

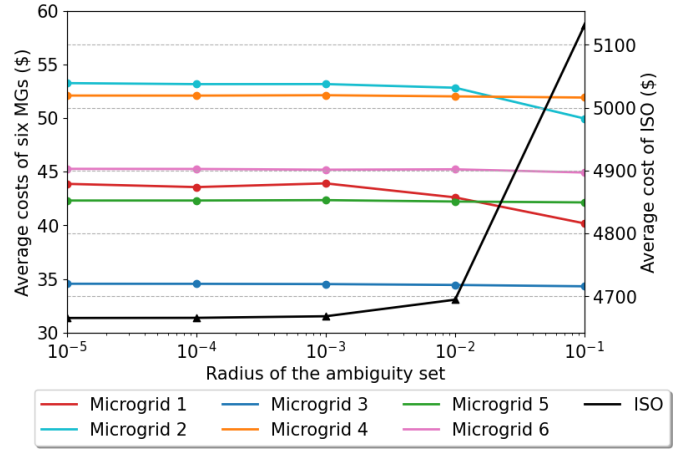


Fig. 6: Average costs of ISO and microgrids with an increasing radius of the ambiguity set

Using the mean values in out-of-sample tests, we calculate the average costs of ISO and six microgrids as the objective functions of models M1 and M2, respectively. Fig. 6 summarizes results in five simulations. The costs of microgrids 1 and 2 reduce when the radius increases from 10^{-3} to 10^{-1} , while the costs of the other four microgrids remain constant with the radius increases. This is because microgrids 1 and 2 have the higher VoLL and tend to be more risk-aware (i.e., bid less) when the ambiguity set becomes more conservative (i.e., larger). The average cost of ISO increases rapidly as the ambiguity set becomes larger, as ISO needs more expensive reserve services from thermal generators.

B. Game results with the increasing number of players

Based on this optimal radius, we simulate the game framework with a varying number of players in the second case study. For each simulation, we increase two microgrid players (from passive net loads at random buses) until the number of players reaches 14. Since microgrids have the same VoLL, we assume their violation rates are also the same (i.e., $\epsilon_0^{ind} = \epsilon_1^{ind} = \dots = \epsilon_n^{ind}$). For comparison, we include two scenarios considering the upper and lower bounds of the equation (13). The scenario for the lower bound (i.e., $\epsilon^{ind} := \frac{\epsilon^{tot}}{N_{MG}}$) denotes C1, and the scenario for the upper bound (i.e., $\epsilon^{ind} := \epsilon^{tot}$) denotes C2. The proposed method C3 aims to find the optimal individual violation rate between two values.

Table II shows the optimized individual violation rates ϵ^{ind} for a different number of players. The value of ϵ^{ind} decreases when the number of players increases since the correlation of microgrids' reserve provisions increases.

TABLE II: The optimized individual violation rates

Players	2	4	6	8	10	12	14
$\epsilon^{ind}(\%)$	20.00	15.02	13.73	12.54	11.10	10.42	9.82

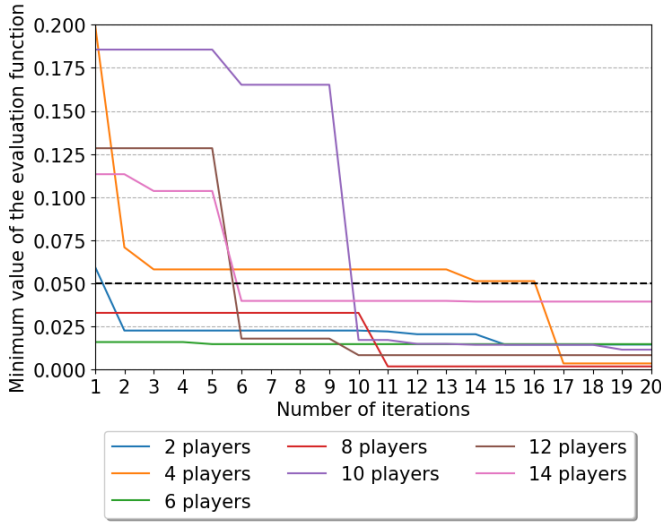


Fig. 7: The convergence of Bayesian optimization in games (Black dash line is the maximum acceptable deviation)

Fig. 7 shows the convergence of Bayesian optimization in different games. The proposed Bayesian optimization allows a maximum number of 20 iterations and accepts the game result when the empirical joint violation rate only deviates from the predefined requirement by less than 0.05. In all experiments, Bayesian optimization can converge to an optimal point within the maximum acceptable deviation (as shown in the black dashed line in Fig. 7), and their computation time is less than 20 mins. Notably, these points are optional to be the global optimum, but they are optimal solutions satisfying both the market clearing time and system reliability requirement.

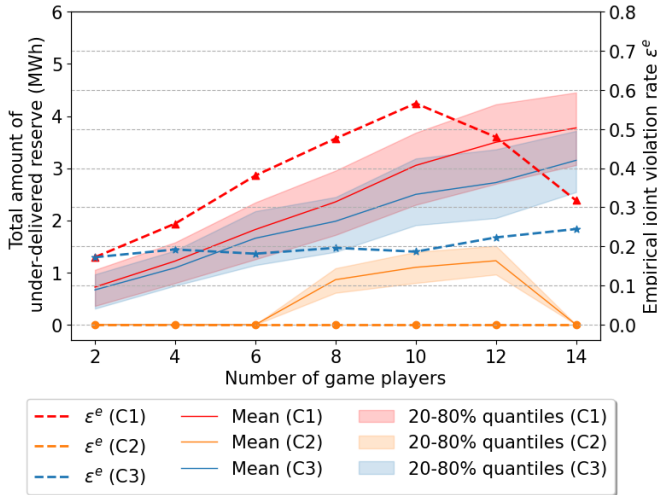


Fig. 8: The total amount of under-delivered reserve and empirical joint violation rates in three scenarios

Fig. 8 shows how the under-delivered reserve and joint

violation rate change in three scenarios. Only the proposed method can regulate the under-delivered reserve and secure the joint violation rate of all microgrids in a game. Using the Bayesian optimization C3 (blue), the total under-delivered reserve increases steadily, and the empirical joint violation rate is regulated at 0.2 ± 0.05 . In scenario C1, the total amount of under-delivered reserve increases rapidly, and the joint violation rate exceeds 0.2 even for the 4-player game and quickly increases to 0.6 in the 10-player game. This means that although C1 using single chance constraints might yield higher profits for microgrids and lower costs for ISO, it is unacceptable from the grid reliability perspective. In scenario C2, on the contrary, the joint violation rate stays close to zero. Neglecting the correlation between players leads to an overly-conservative reserve regulation and almost no reserve bids.

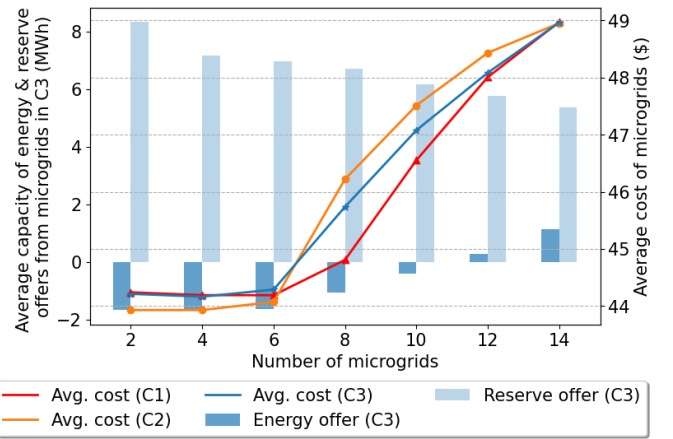


Fig. 9: Average costs of microgrids in three scenarios and their average capacity of energy and reserve offers in C3

Fig. 9 summarizes the average cost of microgrids and the average capacity of their energy and reserve offers in scenario C3. The positive value represents that microgrids sell energy or reserve to the grid and vice versa. There is a trade-off between energy and reserve services, and the reserve capacity of each microgrid decreases as the number of microgrids increases due to market competition.

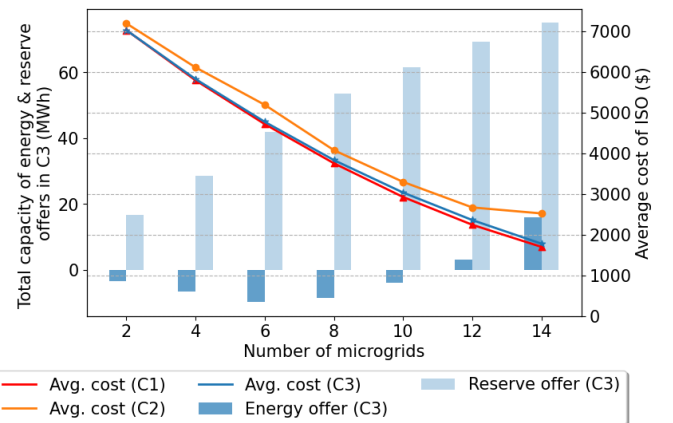


Fig. 10: Average costs of ISO in three scenarios and the total capacity of energy and reserve offers in C3

The game starts with two microgrid players. At first, the average cost of microgrids in scenarios C1 and C3 is more than in C2. As in scenarios C1 and C3, microgrids prefer to invest in the reserve market for higher profits, even if they import power from the grid (as shown in light and dark blue bars). They gain a high load-shedding penalty in return. As the players increase, microgrids reduce their reserve offers due to market competition. The average cost of microgrids in scenarios C1 and C3 becomes lower than in C2. If the number increases to 10 or more, the reserve market becomes saturated, and microgrids need to sell energy for more profits.

Fig. 10 summarizes the cost of ISO and the total capacity of energy and reserve offers from microgrids in scenario C3. The total reserve capacity of microgrids increases, replacing the expensive reserve services from thermal generators (as presented in the light blue bars). Therefore, the cost of ISO straightly decreases with the number of microgrid players increase in the game in all three scenarios. Three scenarios ranked by the ISO's cost are C2, C3, and then C1, which reflect the conservativeness of different system reserve regulations.

VIII. CONCLUSIONS

We propose a DRJCC game to coordinate networked microgrids in competitive power markets. Due to solar power uncertainty, renewable microgrids might breach their day-ahead contracts and under-deliver services in the real-time market. A joint violation event involving multiple microgrids simultaneously could greatly undermine the grid responses to contingencies. In light of reliable reserve provision, a two-stage DRO based on the Wasserstein-metric ambiguity set models the worst-case reserve performance and the expected reserve penalty of each microgrid. A JCC by ISO regulates all the individual day-ahead contracts in the market pool. ISO and microgrids are engaged in a one-leader-multiple-follower game via the MPEC model.

This original DRJCC game is intractable with the unknown individual contract violation allowance. Considering the unspecified correlation in the market game, these optimal violation allowances should effectively regulate the under-delivered reserve and ensure the profits of microgrids in bidding. Instead of enforcing conservative assumptions like the previous works, we design a novel Bayesian optimization method to approach the optimal solutions and solve the market equilibrium iteratively. We include two scenarios to compare with the proposed Bayesian optimization (C3). These two scenarios assume players have the same performances (C1) or no correlation in their reserve provision performances (C2).

Two case studies are performed on a 30-bus network using the CAISO data. The first case study involves six players with different per-unit reserve penalties. The optimal radius of the ambiguity set is identified as $\nu = 0.035$ for a joint violation rate of 0.2. In the second case study, the game is simulated with from 2 to 14 players. Only the Bayesian optimization approach (C3) can converge to the optimal individual violation rates so that the empirical joint violation rates only deviate from the predefined requirement by 0.05 in 20 iterations. In contrast, the other two approaches (C1 and C2) are either

highly unreliable or too strict to reserve bids. The cost analysis of three scenarios (C1-C3) shows the trade-off between bidding in the energy and reserve markets and changing market competition under different numbers of players.

Our future research may be strengthened by considering different market games, such as Nash bargaining or Cournot games, and exploring the applicability of high-dimensional Bayesian optimization.

IX. ACKNOWLEDGEMENT

The authors would like to thank Prof. Pierre Pinson for feedback on the manuscript and Masaki Adachi for feedback on Bayesian optimization. Yifu Ding would like to thank Prof. Malcolm McCulloch's support during the visiting research at Johns Hopkins University.

REFERENCES

- [1] Department for Business, Energy & Industrial Strategy, "Powering our Net Zero Future," Tech. Rep. [Online]. Available: <https://www.gov.uk/government/publications/energy-white-paper-powering-our-net-zero-future>
- [2] M. Keay, J. Rhys, and D. Robinson, "Electricity Market Reform in Britain," in *Evolution of Global Electricity Markets*. Elsevier, 2013, pp. 31–57. [Online]. Available: <https://linkinghub.elsevier.com/retrieve/pii/B978012397891200002X>
- [3] A. Papavasiliou, "Analysis of Distribution Locational Marginal Prices," *IEEE Transactions on Smart Grid*, vol. 9, no. 5, pp. 4872–4882, Sep. 2018. [Online]. Available: <https://ieeexplore.ieee.org/document/7862921/>
- [4] R. Mieth and Y. Dvorkin, "Distribution Electricity Pricing Under Uncertainty," *IEEE Transactions on Power Systems*, vol. 35, no. 3, pp. 2325–2338, May 2020. [Online]. Available: <https://ieeexplore.ieee.org/document/8910409/>
- [5] Z. Zhang, R. Li, and F. Li, "A Novel Peer-to-Peer Local Electricity Market for Joint Trading of Energy and Uncertainty," *IEEE Transactions on Smart Grid*, vol. 11, no. 2, pp. 1205–1215, Mar. 2020. [Online]. Available: <https://ieeexplore.ieee.org/document/8789684/>
- [6] W. Saad, Z. Han, and H. V. Poor, "Coalitional Game Theory for Cooperative Micro-Grid Distribution Networks," in *2011 IEEE International Conference on Communications Workshops (ICC)*. Kyoto, Japan: IEEE, Jun. 2011, pp. 1–5. [Online]. Available: <http://ieeexplore.ieee.org/document/5963577/>
- [7] T. Jiang, C. Wu, R. Zhang, X. Li, H. Chen, and G. Li, "Flexibility Clearing in Joint Energy and Flexibility Markets Considering TSO-DSO Coordination," *IEEE Transactions on Smart Grid*, pp. 1–1, 2022. [Online]. Available: <https://ieeexplore.ieee.org/document/9722366/>
- [8] S. A. Gabriel, A. J. Conejo, J. D. Fuller, B. F. Hobbs, and C. Ruiz, "Equilibria and Complementarity Problems," in *Complementarity Modeling in Energy Markets*. New York, NY: Springer New York, 2013, vol. 180, pp. 127–179, series Title: International Series in Operations Research & Management Science. [Online]. Available: http://link.springer.com/10.1007/978-1-4419-6123-5_4
- [9] S. delaTorre, J. Contreras, and A. Conejo, "Finding Multiperiod Nash Equilibria in Pool-Based Electricity Markets," *IEEE Transactions on Power Systems*, vol. 19, no. 1, pp. 643–651, Feb. 2004. [Online]. Available: <http://ieeexplore.ieee.org/document/1266624/>
- [10] X. Li, C. Li, G. Chen, and Z. Y. Dong, "A Data-driven Joint Chance-constrained Game for Renewable Energy Aggregators in the Local Market," *IEEE Transactions on Smart Grid*, pp. 1–1, 2022. [Online]. Available: <https://ieeexplore.ieee.org/document/9744121/>
- [11] W. Saad, Z. Han, H. Poor, and T. Basar, "Game-Theoretic Methods for the Smart Grid: An Overview of Microgrid Systems, Demand-Side Management, and Smart Grid Communications," *IEEE Signal Processing Magazine*, vol. 29, no. 5, pp. 86–105, Sep. 2012. [Online]. Available: <http://ieeexplore.ieee.org/document/6279592/>
- [12] M. Saguean, N. Kesimal, P. Dessante, and J.-m. Glachant, "Market Power in Power Markets: Game Theory vs. Agent-Based Approach," in *2006 IEEE/PES Transmission & Distribution Conference and Exposition: Latin America*. Caracas, Venezuela: IEEE, 2006, pp. 1–6. [Online]. Available: <http://ieeexplore.ieee.org/document/4104670/>

- [13] P. Sheikhamadi, S. Bahramara, J. Moshtagh, and M. Yazdani Damavandi, "A risk-based approach for modeling the strategic behavior of a distribution company in wholesale energy market," *Applied Energy*, vol. 214, pp. 24–38, Mar. 2018. [Online]. Available: <https://linkinghub.elsevier.com/retrieve/pii/S0306261918300631>
- [14] B. Hobbs, C. Metzler, and J.-S. Pang, "Strategic gaming analysis for electric power systems: an MPEC approach," *IEEE Transactions on Power Systems*, vol. 15, no. 2, pp. 638–645, May 2000. [Online]. Available: <http://ieeexplore.ieee.org/document/867153/>
- [15] K. Bruninx, H. Pandzic, H. Le Cadre, and E. Delarue, "On the Interaction Between Aggregators, Electricity Markets and Residential Demand Response Providers," *IEEE Transactions on Power Systems*, vol. 35, no. 2, pp. 840–853, Mar. 2020. [Online]. Available: <https://ieeexplore.ieee.org/document/8848616/>
- [16] C. Ordoúdis, V. A. Nguyen, D. Kuhn, and P. Pinson, "Energy and reserve dispatch with distributionally robust joint chance constraints," *Operations Research Letters*, vol. 49, no. 3, pp. 291–299, May 2021. [Online]. Available: <https://linkinghub.elsevier.com/retrieve/pii/S0167637721000213>
- [17] Y. Ding, T. Morstyn, and M. D. McCulloch, "Distributionally Robust Joint Chance-Constrained Optimization for Networked Microgrids Considering Contingencies and Renewable Uncertainty," *IEEE Transactions on Smart Grid*, vol. 13, no. 3, pp. 2467–2478, May 2022. [Online]. Available: <https://ieeexplore.ieee.org/document/9709590/>
- [18] M. Mazadi, W. D. Rosehart, H. Zareipour, O. P. Malik, and M. Oloomi, "Impact of wind integration on electricity markets: a chance-constrained Nash Cournot model: CHANCE-CONSTRAINED NASH COURNOT MODEL," *International Transactions on Electrical Energy Systems*, vol. 23, no. 1, pp. 83–96, Jan. 2013. [Online]. Available: <https://onlinelibrary.wiley.com/doi/10.1002/etep.650>
- [19] Y. Matamala and F. Feijoo, "A two-stage stochastic Stackelberg model for microgrid operation with chance constraints for renewable energy generation uncertainty," *Applied Energy*, vol. 303, p. 117608, Dec. 2021. [Online]. Available: <https://linkinghub.elsevier.com/retrieve/pii/S0306261921009788>
- [20] W. Xie, S. Ahmed, and R. Jiang, "Optimized Bonferroni approximations of distributionally robust joint chance constraints," *Mathematical Programming*, vol. 191, no. 1, pp. 79–112, Jan. 2022. [Online]. Available: <https://link.springer.com/10.1007/s10107-019-01442-8>
- [21] W. Chen, M. Sim, J. Sun, and C.-P. Teo, "From CVaR to Uncertainty Set: Implications in Joint Chance-Constrained Optimization," *Operations Research*, vol. 58, no. 2, pp. 470–485, Apr. 2010. [Online]. Available: <http://pubsonline.informs.org/doi/10.1287/opre.1090.0712>
- [22] K. Baker and A. Bernstein, "Joint Chance Constraints in AC Optimal Power Flow: Improving Bounds Through Learning," *IEEE Transactions on Smart Grid*, vol. 10, no. 6, pp. 6376–6385, Nov. 2019. [Online]. Available: <https://ieeexplore.ieee.org/document/8662704/>
- [23] M. Jia, G. Hug, and C. Shen, "Iterative Decomposition of Joint Chance Constraints in OPF," *IEEE Transactions on Power Systems*, vol. 36, no. 5, pp. 4836–4839, Sep. 2021, conference Name: IEEE Transactions on Power Systems.
- [24] A. Arrigo, J. Kazempour, Z. De Greve, J.-F. Toubeau, and F. Vallée, "Embedding Dependencies Between Wind Farms in Distributionally Robust Optimal Power Flow," *IEEE Transactions on Power Systems*, pp. 1–14, 2022. [Online]. Available: <https://ieeexplore.ieee.org/document/9944957/>
- [25] Y. Inatsu, S. Takeno, M. Karasuyama, and I. Takeuchi, "Bayesian optimization for distributionally robust chance-constrained problem," in *International Conference on Machine Learning*. PMLR, 2022, pp. 9602–9621.
- [26] C. Ruiz, A. J. Conejo, J. D. Fuller, S. A. Gabriel, and B. F. Hobbs, "A tutorial review of complementarity models for decision-making in energy markets," *EURO Journal on Decision Processes*, vol. 2, no. 1-2, pp. 91–120, Jun. 2014. [Online]. Available: <https://linkinghub.elsevier.com/retrieve/pii/S2193943821000285>
- [27] R. Gao and A. Kleywegt, "Distributionally Robust Stochastic Optimization with Wasserstein Distance," *Mathematics of Operations Research*, vol. 48, no. 2, pp. 603–655, May 2023. [Online]. Available: <https://pubsonline.informs.org/doi/10.1287/moor.2022.1275>
- [28] J. M. Joyce, "Kullback-Leibler Divergence," in *International Encyclopedia of Statistical Science*, M. Lovric, Ed. Berlin, Heidelberg: Springer Berlin Heidelberg, 2011, pp. 720–722. [Online]. Available: http://link.springer.com/10.1007/978-3-642-04898-2_327
- [29] D. Kuhn, P. M. Esfahani, V. A. Nguyen, and S. Shafieezadeh-Abadeh, "Wasserstein Distributionally Robust Optimization: Theory and Applications in Machine Learning," in *Operations Research & Management Science in the Age of Analytics*, S. Netessine, D. Shier, and H. J. Greenberg, Eds. INFORMS, Oct. 2019, pp. 130–166. [Online]. Available: <http://pubsonline.informs.org/doi/10.1287/educ.2019.0198>
- [30] California ISO, "OASIS - OASIS Prod - PUBLIC - 0." [Online]. Available: <http://oasis.caiso.com/mrioasis/logon.do>
- [31] S. Zymler, D. Kuhn, and B. Rustem, "Distributionally robust joint chance constraints with second-order moment information," *Mathematical Programming*, vol. 137, no. 1-2, pp. 167–198, Feb. 2013. [Online]. Available: <http://link.springer.com/10.1007/s10107-011-0494-7>
- [32] P. Mohajerin Esfahani and D. Kuhn, "Data-driven distributionally robust optimization using the Wasserstein metric: performance guarantees and tractable reformulations," *Mathematical Programming*, vol. 171, no. 1-2, pp. 115–166, Sep. 2018. [Online]. Available: <http://link.springer.com/10.1007/s10107-017-1172-1>
- [33] A. Arrigo, C. Ordoúdis, J. Kazempour, Z. De Grève, J.-F. Toubeau, and F. Vallée, "Wasserstein distributionally robust chance-constrained optimization for energy and reserve dispatch: An exact and physically-bounded formulation," *European Journal of Operational Research*, vol. 296, no. 1, pp. 304–322, Jan. 2022. [Online]. Available: <https://linkinghub.elsevier.com/retrieve/pii/S037721721003271>
- [34] Masaki Adachi, Satoshi Hayakawa, Saad Hamid, Martin Jørgensen, Harald Oberhauser, and Micheal A. Osborne, "SOBER: Scalable Batch Bayesian Optimization and Quadrature using Recombination Constraints." [Online]. Available: <https://arxiv.org/abs/2301.11832>
- [35] B. Shahriari, K. Swersky, Z. Wang, R. P. Adams, and N. de Freitas, "Taking the Human Out of the Loop: A Review of Bayesian Optimization," *Proceedings of the IEEE*, vol. 104, no. 1, pp. 148–175, Jan. 2016. [Online]. Available: <https://ieeexplore.ieee.org/document/7352306/>
- [36] J. Wilson, F. Hutter, and M. Deisenroth, "Maximizing acquisition functions for Bayesian optimization," in *Advances in Neural Information Processing Systems*, S. Bengio, H. Wallach, H. Larochelle, K. Grauman, N. Cesa-Bianchi, and R. Garnett, Eds., vol. 31. Curran Associates, Inc., 2018. [Online]. Available: <https://proceedings.neurips.cc/paper/2018/file/498f2c21688f6451d9f5fd09d53edda7-Paper.pdf>
- [37] Power Systems Test Case Archive, "30 Bus Power Flow Test Case." [Online]. Available: http://labs.ece.uw.edu/pstca/pf30/pg_tca30bus.htm
- [38] UK Power Networks, "Validation of Photovoltaic (PV) Connection Assessment Tool." Tech. Rep. [Online]. Available: <https://www.ofgem.gov.uk/ofgem-publications/93938/pvtoolcdrfnal-pdf>
- [39] Y. Ding and M. McCulloch, "Additive Gaussian process prediction for electrical loads compared with deep learning models," in *Proceedings of the Twelfth ACM International Conference on Future Energy Systems*. Virtual Event Italy: ACM, Jun. 2021, pp. 499–506. [Online]. Available: <https://dl.acm.org/doi/10.1145/3447555.3466592>
- [40] S. Diamond and S. Boyd, "CVXPY: a python-embedded modeling language for convex optimization," *The Journal of Machine Learning Research*, vol. 17, no. 1, pp. 2909–2913, Jan. 2016.
- [41] "scikit-optimize." [Online]. Available: <https://scikit-optimize.github.io/stable/>